

Cite this: *RSC Mechanochem.*, 2026, 3, 201Received 29th June 2025  
Accepted 10th November 2025

DOI: 10.1039/d5mr00088b

rsc.li/RSCMechanochem

# Relationships between milling input energy and chemical reactivity for mechanochemical activation of clays

Alastair T. M. Marsh,<sup>ID</sup>\*<sup>ab</sup> Sreejith Krishnan,<sup>bc</sup> Suraj Rahmon,<sup>bd</sup> Susan A. Bernal<sup>e</sup> and Xinyuan Ke<sup>\*e</sup>

Mechano-chemical activation is of rapidly growing interest for producing cementitious constituents from clays. The chemical reactivity of clay minerals is enhanced during intensive grinding, due to mechano-chemical dehydroxylation and mechanically-induced amorphisation. The most widely used grinding apparatus for laboratory-scale studies is a planetary ball mill. It is still largely unknown whether activation efficacy is critically dependent on any individual milling parameter, or whether trade-offs are possible between different parameters. In this study a first principles approach, previously applied to alloy amorphisation, is adopted to estimate the energy of an individual collision event and the total milling input energy. Using a combination of primary data generated through experiments and secondary data from literature, a set of nearly 100 datapoints was analysed. Rapid increases in chemical reactivity were generally observed for <math><100\text{ kJ g}^{-1}</math> of modelled milling energy input, with a plateau beyond this value. The relationship between chemical reactivity and modelled energy input was well fitted by an exponential type function. For the same modelled milling energy input, a higher gain in chemical reactivity was achieved for the 1:1 clay minerals compared to the 2:1 clay minerals or mixtures of different clay minerals. No strong trends were observed with individual collision energy, with no clear evidence for the existence of a threshold collision energy. The modelled milling input energy was more effective for predicting reactivity increase than measured energy consumption by the mill. Within the ranges tested, increasing ball: powder ratio or rotation speed seemed to be more energetically efficient at increasing reactivity, compared to increasing milling duration. Results from this study can also aid in selection of milling equipment for scaling up this process.

## 1 Introduction

Mechano-chemical activation is a rapidly growing area of technology for increasing the chemical reactivity of clays, with the aim of producing cementitious constituents.<sup>1,2</sup> The principal mechano-chemical reaction undergone by clay minerals during high-energy milling is localized dehydroxylation, *i.e.* the rupture of the O–H bond present in Al–O–H octahedral sites.<sup>3</sup> This leaves an Al–O site, and the migrated proton is believed to subsequently react with other Al–O–H sites to form an H<sub>2</sub>O molecule.<sup>4</sup> In kaolinite, this reaction leads to a progressive change in bulk Al–O coordination from 6-fold to a range of, 4-, 5- and 6-fold.<sup>5</sup> The effects of dehydroxylation on long-range order has primarily been studied for thermally-induced dehydroxylation, and these effects vary depending on mineralogical structure. For 1:1 clay minerals, which have a layer structure consisting of one octahedral alumina sheet and one tetrahedral silica sheet,<sup>6</sup> thermally-induced dehydroxylation results in complete amorphisation.<sup>7</sup> For 2:1 clay minerals, which have a layer structure of one octahedral sheet sandwiched between two tetrahedral silica sheets,<sup>6</sup> thermally-induced dehydroxylation destroys long-range order in the *c*-axis but does not always lead to complete amorphisation.<sup>8</sup>

During high-energy milling of clay minerals, the rupture of O–H bonds (hereafter referred to simply as dehydroxylation) and an increase in structural disorder are observed to occur in parallel.<sup>4,9</sup> For milled clays, it is not yet well-understood what degree of coupling exists between dehydroxylation and amorphisation, and how the extent of dehydroxylation and amorphisation respectively affect dissolution rates in alkaline solutions. At the same time, the specific surface area of clay minerals changes non-monotonically during milling,<sup>10</sup> following three regimes:<sup>11</sup> the ‘Rittinger stage’ of only fracture, the aggregation stage, and the agglomeration stage. It is expected that higher specific surface area of minerals leads to faster dissolution in alkaline solutions, with some dependency on surface morphology<sup>12</sup> and inherent structural order.<sup>13</sup> Nonetheless, whilst fineness can significantly affect the extent

<sup>a</sup>Laboratory of Construction Materials, Ecole Polytechnique Federale de Lausanne, Lausanne 1015, Switzerland. E-mail: alastair.marsh@epfl.ch

<sup>b</sup>School of Civil Engineering, University of Leeds, Leeds LS2 9JT, UK

<sup>c</sup>Department of Civil and Infrastructure Engineering, Indian Institute of Technology Jodhpur, Jodhpur 342011, India

<sup>d</sup>Energy and Environment Directorate, Pacific Northwest National Laboratory (PNNL), Richland, WA 99354, USA

<sup>e</sup>Department of Architecture and Civil Engineering, University of Bath, Bath BA2 78Y, UK. E-mail: x.ke@bath.ac.uk



of dissolution at early ages of reactivity testing (*i.e.* 1 day),<sup>14</sup> the amorphous content is deemed to be the principal determinant of increased reactivity for activated clays at the conventional testing age (*i.e.* 7 days).<sup>15</sup>

Whilst a range of milling apparatus have been used (inc. disk mill,<sup>16</sup> attritor mill<sup>17</sup>), the planetary ball mill is the most widely used apparatus for laboratory scale mechano-chemical activation. Numerous studies at laboratory scale have shown that planetary ball milling is an effective route for inducing changes in the crystalline structure of clay and associated minerals, making them chemically reactive in the presence of an alkaline media. However, a challenge for the development of technology for construction materials production, is to understand more deeply the structure-processing-property-performance relationships for mechano-chemically activated clays. Progress in this topic is hampered by the wide range of variables in three aspects of clay mechano-chemical activation studies: materials features, milling parameters, and performance measurement.

In terms of materials, from the range of clays investigated in the literature so far, the type of clay mineral<sup>18</sup> and its structural characteristics<sup>9</sup> partly determines the relationships between mechano-chemical activation and chemical reactivity. In terms of milling parameters, the planetary ball mill offers a wide range of choices: vessel volume, grinding ball size, material for grinding balls and vessel lining, charge mass, ball to powder ratio, milling rotation speed, and milling duration. Several parametric studies have investigated the effect of varying these parameters,<sup>19–22</sup> which typically conclude with which set of tested parameters the physical, mineralogical and chemical transformation were most effectively achieved. However, there is still a knowledge gap in terms of how interchangeable these parameters are. For example, whether a lower ball-to-powder ratio can be compensated for with a longer milling duration. In terms of performance measurement, there are numerous different ways of assessing the performance of an activated clay, or its pozzolanicity including: strength activity index,<sup>23</sup> lime reactivity test,<sup>24</sup> Chappelle test,<sup>25</sup> Frattini test,<sup>26</sup>  $R^3$  test,<sup>27</sup> modified  $R^3$  test.<sup>28</sup> Whilst these tests are all indicative of an activated clay's chemical reactivity, they are not directly comparable. As a result of so many variables, results from different studies are rarely directly comparable and hence relatively little process has been made so far in gaining a systematic understanding of the energetics of mechano-chemical activation of clays.

Previous studies on the kinetics of mechano-chemical reactions have validated various rate equations for a wide range of different reactions.<sup>29–33</sup> These studies are highly useful from a fundamental perspective, but the typical approach used poses two main limitations regarding their application to the mechano-chemical activation of clay minerals. First, the input parameter varied is typically either milling duration or number of collisions, for a fixed set of milling parameters. Whilst this approach is useful for laboratory studies, the total milling input energy is of greater practical value for assessing suitable activation conditions for a range of milling devices, as well as evaluating trade-offs around duration of milling against the intensity of milling conditions. Second, kinetic laws are

typically investigated with regard to a material property, *e.g.* the extent of reaction for a mechano-chemical synthesis. For activated clays, the material property *per se* (*i.e.* extent of dehydroxylation and amorphisation) is not the exclusive controlling factor of industrial importance, but also the material performance (*i.e.* extent of dissolution in an alkaline environment). Hence, there is a knowledge gap around understanding the energetic trends between clay mineral reactivity and total milling input energy.

To overcome these challenges, this study applies a first principles model for estimating milling input energy from reported experimental parameters. This enables comparison of datasets across numerous studies. A previously validated kinetic model<sup>32</sup> is then adapted and applied for these data of mechano-chemically activated clays. The aims are to gain a more systematic understanding of how variation in milling parameters affects reactivity as cementitious constituents, and how these trends vary between different clay minerals.

## 2 Methodology

The first principles calculation approach used is that developed by Burgio *et al.*<sup>34</sup> This was initially developed for the field of mechanical alloying, and has since been used to develop 'milling maps' for the milling conditions under which alloys can undergo amorphisation.<sup>35</sup> The three core assumptions are: (1) ball motion follows the cataracting regime in which balls are launched from one side of the vessel to the opposite side, due to the ball inertia with respect to the centrifugal forces acting on the vessel itself; (2) only the collisions between launched balls and the vessel wall are considered (collisions between balls are excluded); (3) the frequency of ball launch events (and hence the frequency of collisions) is proportional to the difference in angular velocity between the vessel and the sun wheel. Friction and shear are excluded. A full description of assumptions and approximations is given in the original study,<sup>34</sup> as well as a critical review of its limitations.<sup>36</sup> This approach has since been applied to the topic of mechano-chemical activation of clays by Oze and Mako,<sup>22</sup> but was used only to aid selection of milling parameters, and the calculated values themselves were not published. Whilst other numerical models exist for estimating milling energy, *e.g.* discrete element modelling,<sup>37,38</sup> and the mechanistic UFRJ mill model<sup>39,40</sup> these are far more complex and computationally demanding. For reviews discussing other energetic modelling approaches for planetary ball mills see ref. 41 and 42.

The milling parameters required as model inputs are: vessel diameter, vessel height, grinding ball size, material for grinding balls and vessel lining, charge mass, ball to powder ratio, milling rotation speed, milling duration. The two key outputs of the model are described by eqn (1) and (2). In eqn (1), the individual collision energy (adjusted for extent of ball filling in the vessel),  $\Delta E_b^*$  (J), is calculated from the individual collision energy (*i.e.* the estimated energy dissipated by a single collision between a ball and the vessel wall),  $\Delta E_b$  (J), and the vessel filling factor,  $\phi_b$ . Eqn (1) corresponds to eqn (9) in the original study.<sup>34</sup> In eqn (2), the total modelled milling energy input per unit mass



of powder,  $E_{\text{mod}}$  (Wh  $g^{-1}$ ), is calculated from: the individual collision energy (adjusted for extent of ball filling in the vessel),  $\Delta E_b^*$  (J), obtained *via* eqn (1); the number of balls in the vessel,  $N_b$ ; the frequency of ball launches,  $f_b$  ( $s^{-1}$ ); the duration of milling,  $t$  (h); and, the mass of powder,  $m_p$  (g). Eqn (2) represents a simplified presentation of eqn (10) and (12) in the original study.<sup>34</sup> The calculation spreadsheet used can be found in the associated research dataset.

$$\Delta E_b^* = \varphi_b \cdot \Delta E_b \quad (1)$$

$$E_{\text{mod}} = \frac{\Delta E_b^* \cdot N_b \cdot f_b \cdot t}{m_p} \quad (2)$$

Independently, a similar calculation tool was also developed by Jafter *et al.*,<sup>43</sup> their study adopted the same overall modelling framework proposed by Burgio *et al.*,<sup>34</sup> but used a different approach for calculating individual collision energy to that used in the original study<sup>34</sup> (and also used here). To test the extent of difference between the two models, comparisons of the modelled values for the primary data generated in this study are shown in the SI (Fig. S1 and S2). The modelled milling input energy values calculated with are consistently 40 % higher than those calculated here.<sup>43</sup> The adjustments made in the Jafter *et al.*<sup>43</sup> calculation tool have been described as over-estimating the collision energy compared to the original Burgio *et al.* model.<sup>36</sup> Whilst the choice of model results in differences in absolute values of modelled milling energy (Fig. S1 and S2), it does not affect the relative distribution of the datapoints. The goodness of fit of the modelled curves is the same, whether the values are calculated using the original Burgio *et al.*<sup>34</sup> approach in this study (Fig. 1C and Table 2) or the values calculated using the Jafter *et al.*<sup>43</sup> approach (Fig. S3 and Table S1).

In order to have comparable values of performance, studies were selected which used the  $R^3$  test (standardised as ASTM C1897-20)<sup>27</sup> to measure the chemical reactivity of the activated clays. This is a standardized test which measures the extent to which a given material reacts in a simulated cementitious system, and has the advantage of isolating chemical reactivity from physical effects (which affect the interpretation of mortar-based strength tests).<sup>44</sup> For the  $R^3$  test, a mixture is prepared including the material to be tested (10.1 wt%) along with other constituents that represent a simulated pore solution of a cementitious system: calcium hydroxide (30.3 wt%), calcium carbonate (5.05 wt%) and an alkaline solution (54.5 wt%), prepared by addition of 4 g of potassium hydroxide and 20 g of potassium sulphate to 1 L of deionised water). The extent to which the test material reacts with the other constituents is then determined after 7 days of accelerated curing in a 40 °C environment. Reactivity is measured either by cumulative heat measurements obtained *via* isothermal calorimetry (Method A in ASTM C1897-20) or bound water content measurements (Method B in ASTM C1897-20). Full methodological details can be found within the standard itself. Thresholds have been determined to categorise the reactivity of activated clays as non-reactive, moderately reactive or highly reactive.<sup>45</sup>  $R^3$  literature data were used for both the isothermal calorimetry method and

the bound water content method. The modified  $R^3$  test<sup>28</sup> was used by some studies,<sup>46</sup> but was excluded from consideration here as these values are not directly comparable with the more widely used  $R^3$  test. Similarly, data which used a combination of thermal and mechano-chemical activation processes were excluded as this is not directly comparable with data which solely used mechano-chemical activation.

Original data was generated *via* the activation of three different clays (a kaolinitic clay, K, a montmorillonitic clay, Mt, and a mixed mineral clay, F) using a range of milling parameters (representing 54 data points). For all samples, a Retsch PM100 instrument was used, with a 500 mL stainless steel milling vessel, 2 mm diameter stainless steel grinding balls and a charge of clay material of 15 g. The control parameters were a rotation speed of 550 rpm, a ball : powder ratio of 25, and a duration of 60 minutes; these parameters were varied according to Table 1. The energy consumed by the planetary ball mill during the milling process was measured using a plug meter. 7 day cumulative heat was measured using a TAM Air calorimeter, according to ASTM C1897-20;<sup>27</sup> the single operator coefficient of variation has been established as ~2%, and the multi-laboratory coefficient of variation as ~5%.<sup>47</sup>

Literature data that met the criteria for inclusion (*i.e.* used a planetary ball mill to activate clays and measured chemical reactivity *via* the  $R^3$  test) was obtained using a ‘snowballing’ search strategy, using the keywords of “mechano-chemical activation”, “clay” and “ $R^3$  test”. Five studies met these criteria.<sup>9,18,20,21,48</sup> When required inputs for the model were not found in the published article, these were confirmed with authors *via* personal communication. This gave an additional 51 datapoints, giving a total of 105 datapoints for analysis. Datapoints were grouped by clay mineralogy, in terms of whether the clay consisted of a 1:1 clay mineral, a 2:1 clay mineral or contained a mixture of different mineral clays (as reported in the original studies). Consideration of the detailed

Table 1 Milling parameters varied for the samples tested in this study

Id	Rotation speed (rpm)	Ball : powder ratio	Duration (minutes)
D5	550	25	5
D10	550	25	10
D20	550	25	20
D30	550	25	30
D60	550	25	60
D120	550	25	120
R150	150	25	60
R250	250	25	60
R350	350	25	60
R450	450	25	60
R550	550	25	60
R650	650	25	60
B2	550	2	60
B5	550	5	60
B10	550	10	60
B15	550	15	60
B25	550	25	60
B35	550	35	60



mineralogical changes occurring within the samples (*i.e.* extent of amorphisation, degree of dehydroxylation) is excluded from the scope of the study, as the primary aim is to identify whether broad energetic trends exist across studies. Discussion of such mineralogical changes can be found within the original studies themselves.

Non-linear curve fitting for the  $R^3$  cumulative heat data was carried out using OriginPro 2023b software, applying a damped least squares (Levenberg–Marquardt) iterative algorithm. The tolerance value for a successful fit was set to  $1 \times 10^{-9}$ , and the maximum number of iterations was set to 400. A description of the exponential function used for the non-linear curve fitting (eqn (4)) is given in the Results and discussion section.

The first part of the Results and discussion section investigates relationships between reactivity and modelled milling energy. Because the modelled milling energy can be calculated from the experimental parameters of published studies, this first part of the study uses both primary data and secondary data from previously published literature. The second part of the study investigates relationships between reactivity and measured milling energy. Because the previously published

studies used in the first part did not report measured energy, only primary data was used for the second part of the study.

### 3 Results and discussion

$R^3$  reactivity after 7 days is plotted against modelled milling input energy in Fig. 1A, with datapoints grouped by mineralogy (1 : 1 clay minerals, 2 : 1 clay minerals and mixed mineral clays). A higher 7 day cumulative heat is often associated with a higher chemical reactivity as cementitious constituents.<sup>44,47</sup> Whilst there is considerable scatter in the data, an overall trend can be observed of an initial rapid increase in chemical reactivity with increasing milling input energy ( $<100 \text{ kJ g}^{-1}$ , approximately), followed by a plateau ( $>100 \text{ kJ g}^{-1}$ ) (Fig. 1A). However, there are fewer datapoints for the  $>100 \text{ kJ g}^{-1}$  range.

In previous research, functions have been developed *ab initio* to describe how the extent of a given mechano-chemical reaction proceeds with the number of collisions, and then validated with experimental data.<sup>31</sup> The type of function used depends on the type of reaction: for example, functions developed for mechano-chemical synthesis reactions are distinct depending on whether an intermediate reaction product is involved.<sup>31</sup> The

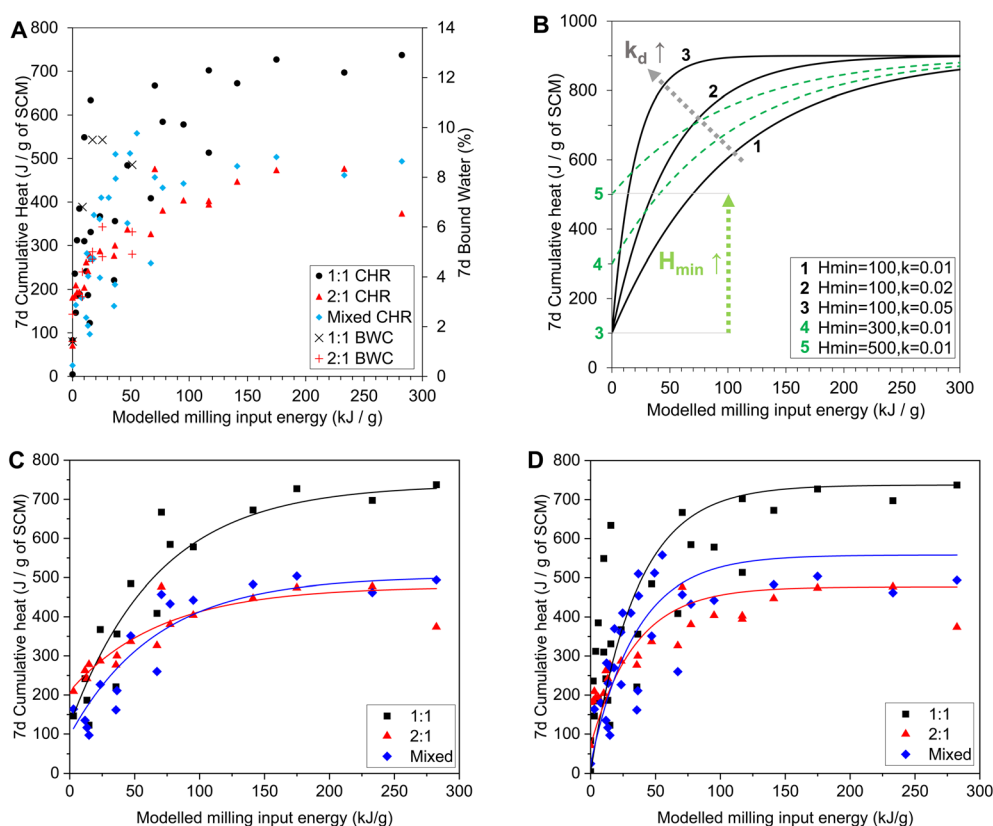


**Fig. 1** (A)  $R^3$  chemical reactivity vs. modelled energy input for all data. Additional data obtained from ref. 9, 18, 20, 21, and 48. "CHR" denotes cumulative heat release data plotted on the left y-axis; "BWC" denotes bound water content data plotted on the right y-axis. The y-axis range maximum is set to  $800 \text{ J g}^{-1}$  of SCM for cumulative heat, and 14% for bound water; these values are considered approximately equivalent, given the close correlation established between the two test methods.<sup>45</sup> (B) Example model curves plotting dummy data, showing the effect of changing parameters  $\Delta H_{min}$  and  $k_d$  (eqn (4)). (C) Fitted curves for the original cumulative heat reactivity data generated in this study, wherein each clay grouping contains only a single source clay. (D) Fitted curves for original and literature-derived data for cumulative heat reactivity, wherein each clay grouping contains  $>1$  source clay.



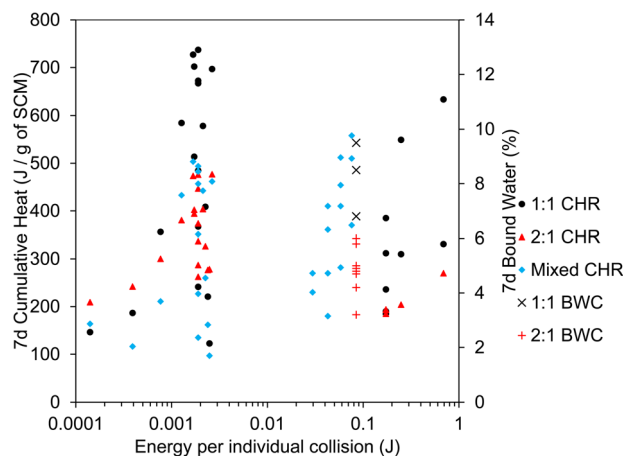


Fig. 2  $R^3$  chemical reactivity vs. energy per individual collision ( $\Delta E_b^*$ ), grouped by mineralogy.

mechano-chemical processes relevant to this study are dehydroxylation and amorphisation; we do not consider that either of these are synthesis reactions. In addition, the 7 day chemical reactivity of activated clays is primarily determined by their amorphous content.<sup>15</sup> Therefore, amongst the range of kinetic models previously developed, the most relevant function to this system was deemed to be the kinetic model which describes progressive amorphisation<sup>32</sup> (experimentally validated on amorphisation of a mixture of Ni and Ti powders<sup>33</sup>). This reaction was successfully modelled using an exponential function. Hence this function type was selected as the most suitable to fit the data in the present study.

The original equation described in ref. 32 is presented here in eqn (3): the degree of amorphisation,  $\alpha$ , is determined from the kinetic constant,  $k_d$  ( $\text{g kJ}^{-1}$ ) and the delivered energy dose,  $D$  ( $\text{kJ g}^{-1}$ ).

$$\alpha = 1 - (1 + k_d D) \exp(-k_d D) \quad (3)$$

This dataset presents a key difference compared to the dataset fitted in ref 32. The measured quantity of interest is a measure of material performance (*i.e.* chemical reactivity), rather than a material property (*i.e.* extent of amorphisation). Whilst extent of amorphisation is limited to between 0 and 1, chemical reactivity varies more freely. For the upper bound, there is no way at present to calculate the theoretical maximum chemical reactivity of a given clay, as this depends on numerous structural and physical aspects (as described in the

Introduction). For the lower bound, the  $R^3$  reactivity of an as-received clay (*i.e.* before milling) is typically low (usually  $<100 \text{ J g}^{-1}$ ) but rarely zero. For this reason, the fitting equation was adapted to suit this dataset in two ways. First, the upper bound was changed from 1 (representing complete amorphisation in the original equation) to the maximum measured chemical reactivity within a given data series. Second, the lower bound was changed from 0 (representing no amorphisation in the original equation) to the minimum measured chemical reactivity within a given data series. The adapted equation is shown in eqn (4). Eqn (4) predicts the 7 day cumulative heat (*i.e.*  $R^3$  reactivity) for a given activated clay,  $H_{7d}$  ( $\text{J g}^{-1}$ ), for a given modelled milling input energy,  $D_{\text{mod}}$  ( $\text{kJ g}^{-1}$ ), as determined from: the maximum measured 7 day cumulative heat for that activated clay,  $H_{\text{max}}$  ( $\text{J g}^{-1}$ ); the minimum measured 7 day cumulative heat for that clay  $H_{\text{min}}$  ( $\text{J g}^{-1}$ ); and, the kinetic constant,  $k_d$  ( $\text{g kJ}^{-1}$ ). Fig. 2B shows how variation in  $k_d$  and  $H_{\text{min}}$  affects the modelled curve, for a constant  $H_{\text{max}}$ .

$$H_{7d} = H_{\text{max}} - ((H_{\text{max}} - H_{\text{min}}) + k_d D_{\text{mod}}) \exp(-k_d D_{\text{mod}}) \quad (4)$$

The primary data generated in this study, in which each clay grouping corresponds to a single source clay, was fitted using eqn (4) (details of fitting procedure are provided in the Methodology section). The fitted curves are shown in Fig. 1C, and the fitting parameters of the fitted curves are reported in Table 2. The  $R^2$  coefficient was  $>0.8$  for all three data series, indicating a reasonable goodness of fit. Whilst there is some clear scatter of datapoints, Fig. 1C suggests that the increase in chemical reactivity of clays with increasing modelled milling energy follows an exponential trend (as described in eqn (4)). This finding is consistent with the kinetic expression originally developed for the extent of amorphisation of metallic powders.<sup>32</sup> The value of the kinetic constant ( $k_d$ ) for all three clay groupings is similar, in the range of  $0.014\text{--}0.015 \text{ g J}^{-1}$  (Table 2). The biggest difference between the clay groupings is the  $H_{\text{max}}$  value; this leads to a larger  $\Delta H$  value (*i.e.* the difference between  $H_{\text{max}}$  and  $H_{\text{min}}$ ) for the 1 : 1 clay ( $614.7 \text{ J g}^{-1}$ ) compared to the 2 : 1 clay ( $267.5 \text{ J g}^{-1}$ ) and the mixed clay ( $406.6 \text{ J g}^{-1}$ ). The energetic implication is that for the same milling input energy, a higher gain in chemical reactivity can be achieved for 1 : 1 clays compared to 2 : 1 clays or mixed clays. Given the goodness of fit, eqn (4) has some potential in helping to optimise the milling input energy for a given clay, if  $H_{\text{max}}$  and  $H_{\text{min}}$  are already known.

Table 2 Fitting parameters for the curves in Fig. 1C (primary data only) and Fig. 1D (primary and secondary data). All parameters are the same as those described in eqn (4).  $\Delta H$  corresponds to the difference between  $H_{\text{max}}$  and  $H_{\text{min}}$ , within each clay grouping data series

Clay grouping	Primary data only					Primary and secondary data				
	$H_{\text{max}}$ ( $\text{J g}^{-1}$ )	$H_{\text{min}}$ ( $\text{J g}^{-1}$ )	$\Delta H$ ( $\text{J g}^{-1}$ )	$k_d$ ( $\text{g J}^{-1}$ )	$R^2$	$H_{\text{max}}$ ( $\text{J g}^{-1}$ )	$H_{\text{min}}$ ( $\text{J g}^{-1}$ )	$\Delta H$ ( $\text{J g}^{-1}$ )	$k_d$ ( $\text{g J}^{-1}$ )	$R^2$
1 : 1 clays	737.3	122.6	614.7	0.0148	0.90	737.3	4.4	732.9	0.0284	0.53
2 : 1 clays	476.8	209.3	267.5	0.0144	0.82	476.8	70.9	405.9	0.0295	0.69
Mixed clays	503.5	96.9	406.6	0.0150	0.86	558.0	25.0	533.0	0.0285	0.57



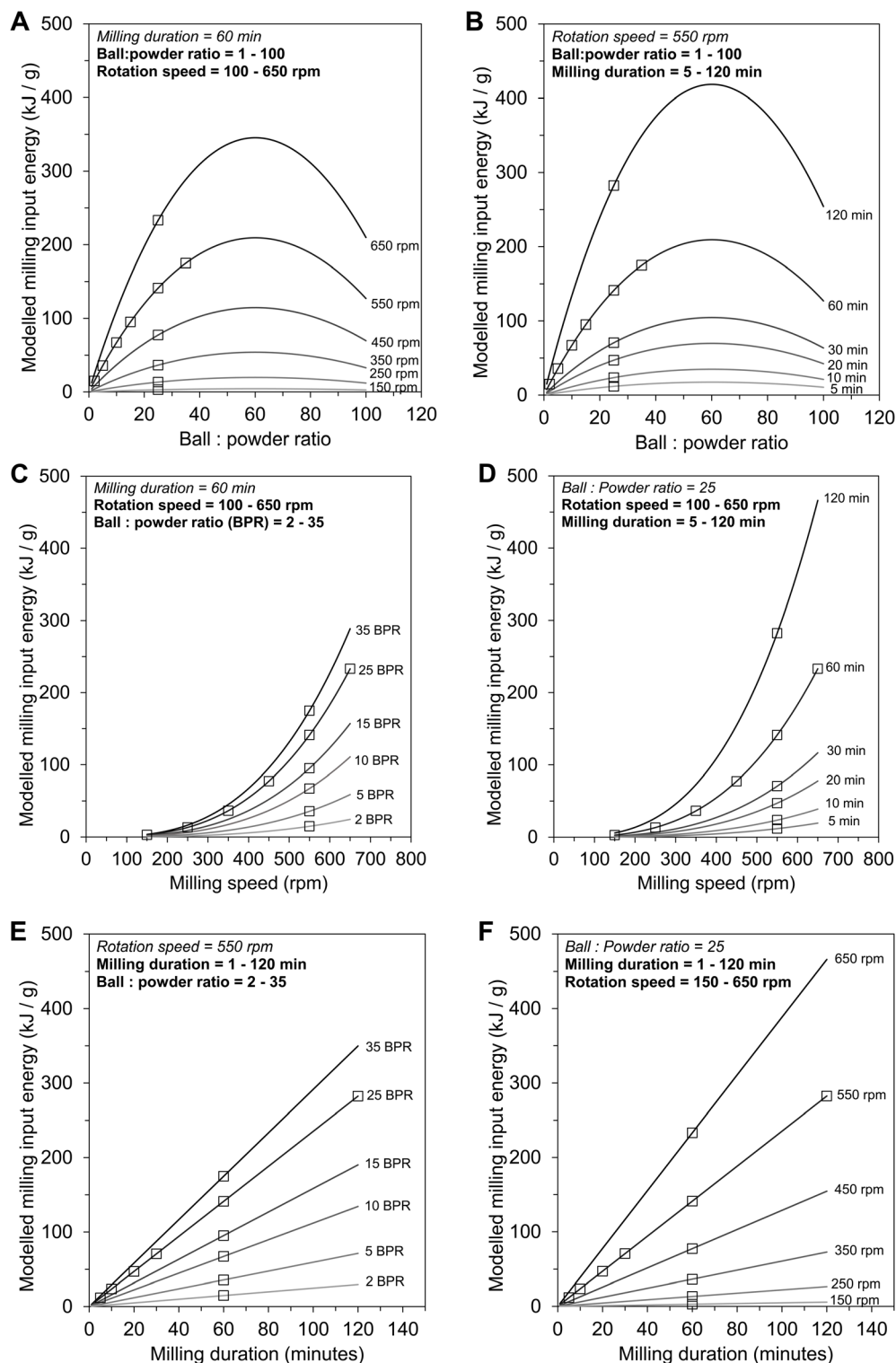


**Fig. 3** Effect on modelled milling energy input ( $\text{kJ g}^{-1}$ ) from changing combinations of continuous variables: (A) ball : powder ratio and rotation speed; (B) ball : powder ratio and milling duration; (C) rotation speed and ball : powder ratio; (D) rotation speed and milling duration; (E) milling duration and ball : powder ratio; (F) milling duration and rotation speed. Reference parameters are: clay charge mass = 15 g; vessel volume = 500 mL; ball diameter = 2 mm; ball and vessel material = stainless steel. The range of rotation speed is limited from 100–650 rpm as this is a typical range possible on laboratory devices. Square markers on the curves represent milling conditions used in this study, as described in Table 1.

The same fitting exercise was carried out for the combined set of primary and secondary data, again grouped by clay mineral (Fig. 1D, Table 2). The  $R^2$  coefficient of the fitted curves

decreased for all clay groupings (0.53–0.69), compared to the fitted curves for the primary data only (0.82–0.90). The data-points still broadly plateau beyond a modelled milling input



energy of  $100 \text{ kJ g}^{-1}$ ; however, variation between clays (primarily in terms of their  $H_{\text{max}}$  and  $H_{\text{min}}$  values) leads to a much greater scatter of data. This degree of scatter precludes the use of eqn (4) for *ab initio* predictions of chemical reactivity for a given clay without prior knowledge of  $H_{\text{max}}$  and  $H_{\text{min}}$ .

An outstanding question around the mechano-chemical activation of clays is whether a minimum impact energy (per individual collision) is needed to achieve dehydroxylation and/or amorphisation; and whether this varies across different clay mineral types. In a general sense, if the individual impact energy is sufficiently high, then a single collision can be enough for the mechano-chemical reaction to take place.<sup>49</sup> The minimum individual impact energy required for a mechano-chemical reaction has been inferred from experiments in a vibratory ball mill using a single ball, by using different impact energies and extrapolating the value for which the rate constant becomes zero.<sup>50–52</sup> Previously established values for the minimum individual impact energy are: 0.017 J for the hcp to fcc transformation of Co powder,<sup>50</sup> 0.025 J for the reaction of Ti and C to form TiC,<sup>51</sup> and 0.005–0.024 J for the trimerisation of bis(dibenzoylmethanato)nickel(II) (the value within this range depended on ball material and diameter).<sup>52</sup> Plotting  $R^3$  chemical reactivity against  $\Delta E_b^*$  (eqn (1)) shows that calculated  $\Delta E_b^*$  spans four orders of magnitude across the dataset (Fig. 2). For both below and above the range of minimum impact energies for other reactions cited above (*i.e.* 0.005–0.025 J), a wide range of chemical reactivity is achieved with some exceeding  $500 \text{ J g}^{-1}$ . This indicates that the minimum impact energy, as estimated here for clay mineral dehydroxylation and/or amorphisation in a planetary ball mill, is lower than those in the previous cited studies. For datapoints where the individual impact energy is  $\leq 0.001 \text{ J}$ , only low chemical reactivity ( $<350 \text{ J g}^{-1}$ ) was obtained – this could indicate the existence of a minimum impact energy within this range, although few studies collected datapoints in this range.

However, an additional factor is the rise in ambient temperature during planetary ball milling, which can reach around  $80 \text{ }^\circ\text{C}$ <sup>18</sup> and higher for this range of conditions. Mechanochemical reaction kinetics have a strong dependence on the temperature within the milling vessel.<sup>53</sup> The data presented here are hence expected to represent coupled effects, deriving from differences both in individual collision energy and in ambient temperature. On a practical level, a broad range of chemical reactivity values was obtained at both the higher ( $<1 \text{ J}$ ) and lower ( $>0.001 \text{ J}$ ) range of collision energies. This suggests that less intensive milling conditions (in terms of individual collision energy) can generally be compensated for by longer milling durations. A key difference between a planetary ball mill (as used in this study) and a vibratory ball mill using a single ball (as used in the cited previous studies investigating minimum impact energy) may be the shear stresses that powders are exposed to, in addition to normal stresses from impacts.<sup>38</sup> Shear stresses in combination with normal impact stresses are likely to play an important role in aspects of mechano-chemical reactions,<sup>50</sup> as already shown in tribochemical investigations<sup>54</sup> and through shear-induced amorphisation in geological materials.<sup>55</sup> This combination of

applied stresses may therefore obscure the detection of a minimum collision energy in a planetary ball mill.

Using a reference set of milling parameters based on the values in Table 1, the model was used to test the effect of varying the three key continuous variables: ball : powder ratio (Fig. 3A and B), rotation speed (Fig. 3C and D) and milling duration (Fig. 3E and F). Increasing ball : powder ratio increases modelled milling input energy up to a value of  $\sim 60$  (Fig. 3A and B). Beyond  $\sim 60$ , the reduction in modelled individual collision energy (due to an increased vessel filling factor, eqn (1)) overcomes the effect of an increased number of collisions, leading to a decrease in modelled milling input energy. Increasing rotation speed leads to a polynomial increase in modelled input energy, due to the dependence of individual collision energy on the velocity of launched balls (*i.e.*,  $E = mv^2$ ), with an additional contribution from increased collision frequency (Fig. 3C and D). The increase of modelled milling input energy with longer milling duration is linear (Fig. 3E and F). The mathematical functions of the modelled dependencies varies between these three parameters. Nonetheless, these modelled trends together support the experimental observations in Fig. 1 and 2: that the extent of mechano-chemical activation largely depends on total milling input energy; and, lower values of one milling parameter can be compensated for (to some extent) by higher values of another milling parameter.

The energy transferred into the milled material is of fundamental interest for understanding the relationships between milling parameters and chemical reactivity. In parallel, the

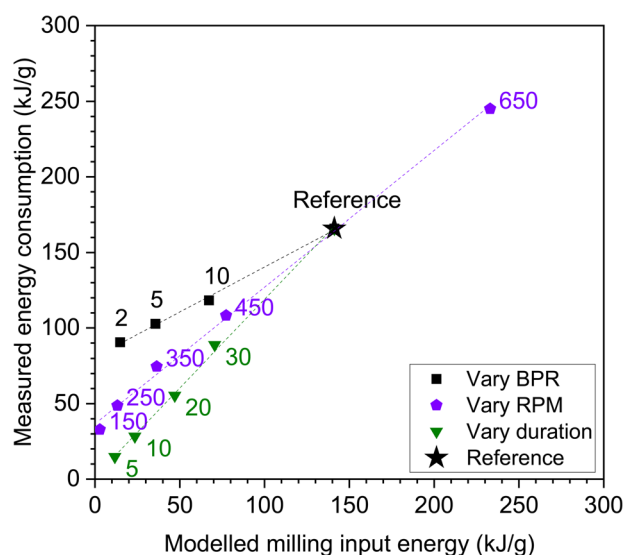


Fig. 4 Measured energy consumption vs. modelled energy input, for data generated in this study. Each series corresponds to a series of milling parameters varying one independent parameter: BPR = ball : powder ratio; RPM = rotation speed (rpm); duration = duration of milling (minutes). The reference point corresponds to the control set of milling parameters, *i.e.* ball : powder ratio = 25, rotation speed = 550 rpm, duration = 60 minutes. The label on each datapoint corresponds to the value of the independent variable in that series, *e.g.* '10' in the 'vary BPR' series corresponds to a BPR of 10. A linear curve has been fitted to each data series.



Table 3 Fitting parameters for the linear curves in Fig. 4

Parameter varied	Gradient	y-intercept (kJ g <sup>-1</sup> )	R <sup>2</sup>
Ball : powder ratio (BPR)	0.6	80.8	0.997
Rotation speed (RPM)	0.9	36.6	0.997
Duration	1.2	1.6	0.998

actual energy consumed by the apparatus during milling is of practical interest for determining the embodied energy of the mechano-chemically activated clay. The magnitude of values for measured energy consumption are broadly comparable with those reported by Oze and Mako<sup>22</sup> for similar milling parameters, albeit using a Fritsch Pulverisette 6 planetary ball mill (rather than a Retsch PM100). Plotting the measured energy consumption against the modelled energy input (Fig. 4), there is an overall positive correlation albeit with significant spread in the lower ranges (especially  $\leq 50$  kJ g<sup>-1</sup> of modelled energy). In general, the measured energy consumption is similar to the modelled energy consumption.<sup>34</sup>

Each data series in Fig. 4 shows the effect of varying one milling parameter on the modelled milling energy input and measured energy consumption, whilst keeping all other parameters constant. Each data series can be fitted well with a linear curve, with R<sup>2</sup> values > 0.99 (Table 3). The projected y-intercept is close to 0 kJ g<sup>-1</sup> for the 'vary duration' series, and higher for 'vary RPM' series (36.6 kJ g<sup>-1</sup>) and highest for the 'vary BPR' series (80.8 kJ g<sup>-1</sup>). The implication from these y-intercept values is that in the range of modelled energy input <100 kJ g<sup>-1</sup>, it is instrumentally less efficient to decrease ball : powder ratio and/or rotation speed. Viewed the other way, it is instrumentally more efficient to use a higher ball : powder ratio and/or a faster rotation speed (and a shorter milling duration) to achieve a given modelled milling input energy.

If chemical reactivity is then plotted against measured energy consumption (only for the original data generated in this study, Fig. 5A), the spread of datapoints is extremely broad albeit with an overall weak positive trend. The spread of

reactivity data in Fig. 5A is greater than the same reactivity data when plotted against modelled milling input energy in Fig. 1C: this indicates that the modelled milling input energy is more accurate as a predictor of reactivity evolution than measured energy consumption.

To investigate the reasons behind this wider spread, the datapoints for the 1:1 clay were grouped by the milling parameter varied (Fig. 5B). Similar to Fig. 4, clear trends were visible for the variation of each milling parameter. If the energy consumption is reduced from the reference datapoint, a reduction in ball : powder ratio leads to the sharpest drop in reactivity, followed by a reduction in rotation speed, with a reduction in duration having the least effect. Viewed the other way, one can infer that ball : powder ratio is the most significant factor for increasing reactivity, followed by rotation speed and then duration. Ball : powder ratio<sup>56</sup> and milling frequency<sup>57</sup> have separately been highlighted as influential parameters for increasing the extent of a mechano-chemical reaction at a given milling duration; this analysis experimentally shows their influence relative to each other.

To investigate the issue of energetic efficiency in more detail, an 'activation efficiency' metric was calculated (eqn (5)). This gives a quantitative measure for the extent to which additional energy consumed during the milling process results in improved chemical reactivity in the activated clay. The higher the value, the more energetically efficient that set of milling parameters is considered to be.

$$\text{Activation efficiency (J kJ}^{-1}\text{)} = \frac{\text{chemical reactivity (J g}^{-1}\text{ of SCM)}}{\text{energy consumed during milling (kJ g}^{-1}\text{)}} \quad (5)$$

Even for activated clays produced from the same as-received clay, differences in activation efficiency of over a factor of 5 were observed (Fig. 6A). For example, two milled montmorillonitic (Mt prefix) clays Mt\_D5 and Mt\_B5 had 7d cumulative heat values of 262.4 and 276.7 J g<sup>-1</sup> of SCM respectively, but Mt\_D5

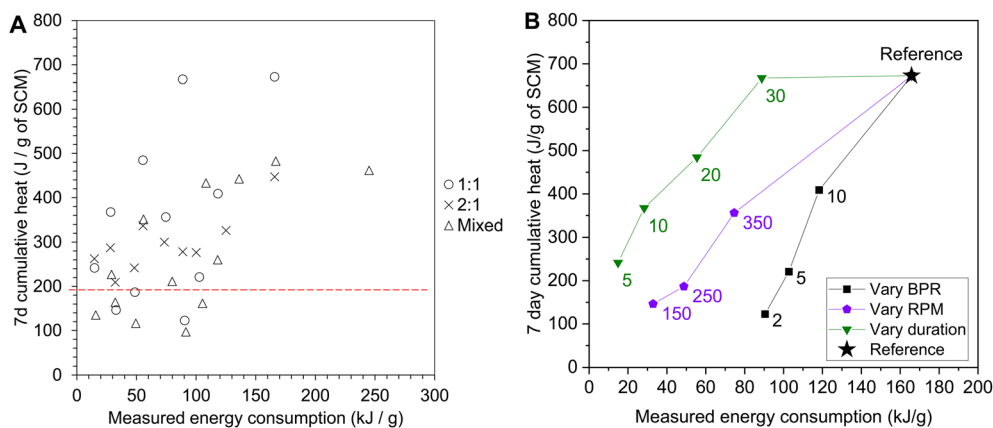


Fig. 5 (A) R<sup>3</sup> chemical reactivity vs. measured energy consumption for the data generated in this study. The dashed line at 190 J g<sup>-1</sup> of SCM corresponds to the threshold for a 'moderately reactive' activated clay.<sup>45</sup> (B) Datapoints for the 1 : 1 clay only, with each data series corresponding to the milling parameter being varied individually (same abbreviations as used in Fig. 4).



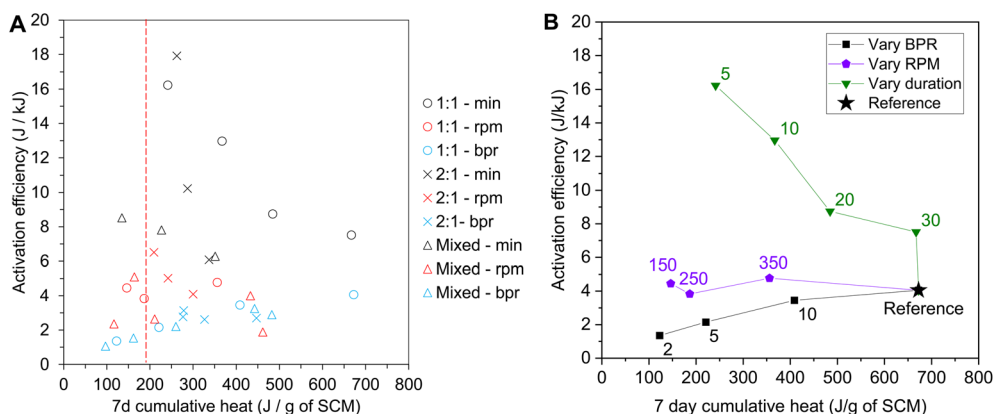


Fig. 6 (A) Activation efficiency metric vs.  $R^3$  chemical reactivity. The series suffixes represent the series varying each continuous milling parameter, as listed in Table 1: "min" = milling duration; "rpm" = rotation speed; "bpr" = ball : powder ratio. The dashed line at  $190 \text{ J g}^{-1}$  of SCM corresponds to the threshold for a 'moderately reactive' activated clay.<sup>45</sup> (B) Datapoints for the 1 : 1 clay only, with each data series corresponding to the milling parameter being varied individually (same abbreviations as used in Fig. 4).

had an activation efficiency of  $17.9 \text{ J kJ}^{-1}$  compared to  $2.8 \text{ J kJ}^{-1}$  for Mt\_B5. 70% of the samples tested (23 out of 40) had an activation efficiency in the range of 2–7  $\text{J kJ}^{-1}$ . A weak trend across all the clay types investigated was a tendency for the highest activation efficiencies to occur in the reactivity range of 200–400  $\text{J g}^{-1}$  of SCM, with a decrease in activation efficiency to achieve higher levels of reactivity. In other words, it is energetically less efficient to increase the chemical reactivity of a given clay beyond a certain level. This energetic observation is consistent with a previous study, which found highest reactivity in kaolinitic clays occurred before complete amorphisation was achieved.<sup>22</sup>

When data for the 1:1 clay is grouped by the milling parameter varied (Fig. 6B), distinct trends are again evident for each milling parameter. Comparing the different routes to achieve a higher chemical reactivity by changing milling parameters: increasing milling duration is energetically inefficient; increasing ball : powder ratio makes milling more energetically efficient, and activation efficiency seems largely unaffected by varying the rotation speed. These trends are likely a combination of the differences in modelled milling input energy and the different loss factors arising in the planetary ball mill equipment itself.

Embodied energy is a key concern in the cement industry; a common question for proponents of mechano-chemical activation is around the embodied energy of mechano-chemically activated clays. Whilst the values here are useful for understanding trends, it is reiterated that the planetary ball mill is only suitable for laboratory scale production given limitations around industrial upscaling.<sup>58,59</sup> Given the laboratory scale context of this processing method, it is not considered meaningful to compare these figures to literature values for the embodied energy of thermal activation. For example, the embodied energy of activated clays was drastically reduced simply by using a laboratory planetary ball mill configuration which allowed two milling jars to be stacked on top of each

other.<sup>22</sup> Nonetheless, mechano-chemical activation is not restricted to the planetary ball mill. Mechano-chemical activation of several minerals (*e.g.* quartz) can be achieved across different grinding devices.<sup>60</sup> Understanding the criteria for mechano-chemical activation in laboratory mills, particularly the dependencies around total input energy and the threshold individual impact energy, can help to inform the selection of scalable grinding devices and suitable grinding conditions.

A limitation of this first principles approach to modelling milling input energy is the simplicity of its assumptions. Crucially, the model assumes the energy is only transferred to the material through impact collisions,<sup>34</sup> whereas it is known that friction and shearing forces are important in planetary ball milling.<sup>38</sup> Nonetheless, this modelling approach is useful for establishing a common metric to compare across diverse sets of milling parameters, and establishing a threshold behind which further reactivity increases are asymptotic.

## 4 Recommendations for experimental reporting

A challenge in mechanochemistry is that frequently, insufficient information about milling conditions is reported for experiments to be repeatable.<sup>61</sup> Furthermore, the lack of sufficient methodological information limits the extent to which existing literature data can be used to feed first principles models (such as that used in this study). We recommend that the following milling parameters should be reported by all studies on the mechano-chemical activation of clays:

- Vessel diameter (mm).
- Vessel height (mm).
- Grinding ball diameter (mm).
- Material for grinding balls and vessel lining.
- Mass of material (being milled) (g).
- Mass of grinding balls (g).
- Milling rotation speed (rpm).



- Milling duration (minutes).

We also recommend that researchers routinely measure the energy consumed during each milling run. This can be carried out using a simple plug meter. More sophisticated ways of measuring energy consumption exist for some planetary ball mills. For example, the Retsch PM100 and PM200 models include a function to separately measuring the idling energy (corresponding to losses) and the comminution energy.<sup>62</sup> In mills which do not feature these dedicated functions, measuring the energy consumed by spinning an empty vessel may help to estimate the energy dissipated through friction at a given rotation speed.

## 5 Conclusions

This study has applied a first principles approach to estimate milling energy in a planetary ball mill, and analysed nearly 100 data point across original data and secondary data from previous studies. This has brought new insights into how variation in milling parameters influences the mechano-chemical activation of clays. The five key findings are:

(1) Increases in chemical reactivity with increasing modelled milling input energy can be fitted well using an exponential type function, previously developed for amorphisation of metallic powders.

(2) A plateau exists beyond approximately 100 kJ g<sup>-1</sup>, at which there is little further increase in chemical reactivity despite higher milling energy.

(3) Modelled milling input energy is more effective for predicting reactivity increases compared to measured milling input energy.

(4) Increasing ball : powder ratio and rotation speed seem to be more energetically efficient for increasing chemical reactivity, compared to increasing duration of milling.

(5) There is no clear evidence for a threshold individual collision energy for mechano-chemical dehydroxylation in the planetary ball mill within the range of conditions tested so far.

These findings so far are largely consistent across different clay mineralogies. However, they will need to be validated with 100 s of additional datapoints for different clays and across different laboratories; and also, across a wider variety of materials beyond clays (e.g. slags, silicate minerals). The practical implications of these findings are to help researchers select milling parameters for laboratory mechano-chemical activation studies. For example, by avoiding sets of parameters for which the modelled milling input energy is far below the level expected to achieve effective mechano-chemical activation. Or alternatively, to study a wide range of milling parameters to establish the boundaries of which conditions are not effective, in addition to the range of what does work well. The calculation model developed by Burgio *et al.*<sup>34</sup> and used here is arithmetically complex but not computationally demanding. Validation of this simple model for planetary ball mills also opens up the opportunity to develop other simple models for milling apparatus which are more suited for up-scaled production, e.g. attritor mills. There is much potential for research in mechano-chemical activation to adopt this approach, both for

understanding trends within datasets, and to aid with selection of milling parameters. In parallel, applying experimental approaches for measuring the activation energy<sup>63</sup> and the minimum impact energy<sup>52</sup> to the mechano-chemical dehydroxylation of clay minerals will improve our knowledge around their reaction kinetics.

## Author contributions

A. T. M. Marsh: conceptualisation; methodology; investigation; formal analysis, writing – original draft; S. Krishnan: data curation, investigation; S. Rahmon: investigation; S. A. Bernal: funding acquisition; project administration, supervision, writing – review & editing; X. Ke: funding acquisition; writing – review & editing.

## Conflicts of interest

There are no conflicts of interest to declare.

## Data availability

The data supporting this article are available at <https://doi.org/10.5281/zenodo.17771208>. Supplementary information is available. See DOI: <https://doi.org/10.1039/d5mr00088b>.

## Acknowledgements

This study was sponsored by the Industrial Decarbonisation Research and Innovation Centre (IDRIC), project MIP 8.7 under the UK Engineering and Physical Sciences Research Council (EPSRC) grant EP/V027050/1. The participation of A. T. M. Marsh and S. A. Bernal was funded under EP/W021811/1 (EPSRC grant) and the EPSRC Early Career Fellowship (EP/R001642/1). Thanks are given to Jofre Manosa and Gilles Plusquellec for providing additional experimental information about milling parameters used in their studies.

## References

- 1 I. Tole, K. Habermehl-Cwirzen and A. Cwirzen, *Mineral. Petrol.*, 2019, **113**, 449–462.
- 2 D. Meng, J. N. Yankwa Djobo, I. P. Segura, R. C. Kaze, C. Kuenzel and N. Ranjbar, *Mater. Today*, 2025, DOI: [10.1016/j.mattod.2025.11.024](https://doi.org/10.1016/j.mattod.2025.11.024).
- 3 J. G. Miller and T. D. Oulton, *Clays Clay Miner.*, 1970, **18**, 313–323.
- 4 R. L. Frost, É. Makó, J. Kristóf, E. Horváth and J. T. Klopogge, *J. Colloid Interface Sci.*, 2001, **239**, 458–466.
- 5 J. Klopogge, in *Spectroscopic Methods in the Study of Kaolin Minerals and Their Modifications*, ed. J. Klopogge, Springer International Publishing, Cham, 2019, pp. 161–241.
- 6 M. F. Brigatti, E. Galan, and B. K. G. Theng, in *Developments in Clay Science*, ed. F. Bergaya, B. K. G. Theng, and G. Lagaly, Elsevier, 2006, vol. 1, pp. 19–86.
- 7 D. Massiot, P. Dion, J. F. o. Alcover and F. Bergaya, *J. Am. Ceram. Soc.*, 1995, **78**, 2940–2944.



- 8 N. Garg and J. Skibsted, *J. Phys. Chem. C*, 2014, **118**, 11464–11477.
- 9 A. T. M. Marsh, A. P. Brown, H. M. Freeman, A. Neumann, B. Walkley, H. Pendrowski and S. A. Bernal, *J. Mater. Chem. A*, 2024, **12**, 24260–24277.
- 10 É. Kristóf, A. Z. Juhász and I. Vassányi, *Clays Clay Miner.*, 1993, **41**, 608–612.
- 11 L. Opoczky, *Powder Technol.*, 1977, **17**, 1–7.
- 12 A. A. Jeschke and W. Dreybrodt, *Geochim. Cosmochim. Acta*, 2002, **66**, 3055–3062.
- 13 S. H. Sutherland, P. A. Maurice and Q. Zhou, *Am. Mineral.*, 1999, **84**, 620–628.
- 14 S. Blotvogel, A. Ehrenberg, L. Steger, L. Doussang, J. Kaknics, C. Patapy and M. Cyr, *Cem. Concr. Res.*, 2020, **130**, 105998.
- 15 S. Overmann, A. Vollpracht and T. Matschei, *Materials*, 2024, **17**(2), 312.
- 16 H. Niu, L. R. Adrianto, A. G. Escobar, V. Zhukov, P. Perumal, J. Kauppi, P. Kinnunen and M. Illikainen, *J. Sustain. Metall.*, 2021, **7**, 1575–1588.
- 17 P. Zhao, A. Ozersky, A. Khomyakov and K. Peterson, *Cement Concr. Compos.*, 2025, **160**, 106034.
- 18 V. A. Baki, X. Ke, A. Heath, J. Calabria-Holley, C. Terzi and M. Sirin, *Cem. Concr. Res.*, 2022, **162**, 106962.
- 19 I. Tole, K. Habermehl-Cwirzen, M. Rajczakowska and A. Cwirzen, *Materials*, 2018, **11**(10), 1860.
- 20 J. Mañosa, A. Alvarez-Coscojuela, J. Marco-Gibert, A. Maldonado-Alameda and J. M. Chimenos, *Appl. Clay Sci.*, 2024, **250**, 107266.
- 21 G. Plusquellec, O. Chaudhari, E. L'Hôpital and K. Malaga, *Presented in Part at the the 16th International Congress on the Chemistry of Cement*, Bangkok, 2023.
- 22 C. Óze and É. Makó, *Minerals*, 2023, **13**, 915.
- 23 ASTM, *Standard Test Methods for Sampling and Testing Fly Ash or Natural Pozzolans for Use in Portland-Cement Concrete*, ASTM International, West Conshohocken, PA, 2022, C311-22.
- 24 BIS, *Method of Test for Pozzolan Materials*, Bureau of Indian Standards, New Delhi, India, 1967, IS-1727.
- 25 AFNOR, *Addition for Concrete-Metakaolin-Specifications and Conformity Criteria*, Association Française de Normalisation, La Plaine Saint-Denis, France, 2012, NF P18-513.
- 26 BSI, *Methods of Testing Cement Pozzolanicity Test for Pozzolan Cement*, British Standards Institution, London, UK, 2011, BS EN 196-5:2011.
- 27 ASTM, *Standard Test Methods for Measuring the Reactivity of Supplementary Cementitious Materials by Isothermal Calorimetry and Bound Water Measurements*, ASTM International, West Conshohocken, PA, 2020, C1897-20.
- 28 P. Suraneni and J. Weiss, *Cement Concr. Compos.*, 2017, **83**, 273–278.
- 29 R. J. Allenbaugh, T. M. Ariagno and J. Selby, *RSC Mechanochem.*, 2025, **2**, 30–36.
- 30 M. Carta, F. Delogu and A. Porcheddu, *Phys. Chem. Chem. Phys.*, 2021, **23**, 14178–14194.
- 31 M. Carta, E. Colacino, F. Delogu and A. Porcheddu, *Phys. Chem. Chem. Phys.*, 2020, **22**, 14489–14502.
- 32 F. Delogu and L. Takacs, *J. Mater. Sci.*, 2018, **53**, 13331–13342.
- 33 F. Delogu, L. Schiffini and G. Cocco, *Philos. Mag. A*, 2001, **81**, 1917–1937.
- 34 N. Burgio, A. Iasonna, M. Magini, S. Martelli and F. Padella, *Il Nuovo Cimento D*, 1991, **13**, 459–476.
- 35 B. S. Murty, M. Mohan Rao and S. Ranganathan, *Acta Metall. Mater.*, 1995, **43**, 2443–2450.
- 36 G. I. Peterson, *Angew. Chem., Int. Ed.*, 2025, **64**, e202512324.
- 37 H. Mio, J. Kano, F. Saito and K. Kaneko, *J. Mater. Sci. Eng. A*, 2002, **332**, 75–80.
- 38 S. Rosenkranz, S. Breitung-Faes and A. Kwade, *Powder Technol.*, 2011, **212**, 224–230.
- 39 L. M. Tavares and R. M. de Carvalho, *Miner. Eng.*, 2009, **22**, 650–659.
- 40 V. A. Rodriguez, L. Ribas, A. Kwade and L. M. Tavares, *Powder Technol.*, 2023, **429**, 118901.
- 41 C. F. Burmeister and A. Kwade, *Chem. Soc. Rev.*, 2013, **42**, 7660–7667.
- 42 H. X. Khoa, S. Bae, S. Bae, B.-W. Kim and J. S. Kim, *J. Powder Mater.*, 2014, **21**, 155–164.
- 43 O. F. Jaffer, S. Lee, J. Park, C. Cabanetos and D. Lungerich, *Angew. Chem., Int. Ed.*, 2024, **63**, e202409731.
- 44 F. Avet, R. Snellings, A. Alujas Diaz, M. Ben Haha and K. Scrivener, *Cem. Concr. Res.*, 2016, **85**, 1–11.
- 45 D. Londono-Zuluaga, A. Gholizadeh-Vayghan, F. Winnefeld, F. Avet, M. Ben Haha, S. A. Bernal, Ö. Cizer, M. Cyr, S. Dolenc, P. Durdzinski, J. Haufe, D. Hooton, S. Kamali-Bernard, X. Li, A. T. M. Marsh, M. Marroccoli, M. Mrak, Y. Muy, C. Patapy, M. Pedersen, S. Sabio, S. Schulze, R. Snellings, A. Telesca, A. Vollpracht, G. Ye, S. Zhang and K. L. Scrivener, *Mater. Struct.*, 2022, **55**, 142.
- 46 A. Hazarika, L. Huang and A. Babaahmadi, *Mater. Struct.*, 2024, **57**, 68.
- 47 F. Avet, X. Li, M. Ben Haha, S. A. Bernal, S. Bishnoi, Ö. Cizer, M. Cyr, S. Dolenc, P. Durdzinski, J. Haufe, D. Hooton, M. C. G. Juenger, S. Kamali-Bernard, D. Londono-Zuluaga, A. T. M. Marsh, M. Marroccoli, M. Mrak, A. Parashar, C. Patapy, M. Pedersen, J. L. Provis, S. Sabio, S. Schulze, R. Snellings, A. Telesca, M. Thomas, F. Vargas, A. Vollpracht, B. Walkley, F. Winnefeld, G. Ye, S. Zhang and K. Scrivener, *Mater. Struct.*, 2022, **55**, 92.
- 48 A. T. M. Marsh, S. Krishnan and S. A. Bernal, *Cem. Concr. Res.*, 2024, **181**, 107546.
- 49 M. Carta, L. Vugrin, G. Miletić, M. J. Kulcsár, P. C. Ricci, I. Halasz and F. Delogu, *Angew. Chem., Int. Ed.*, 2023, **62**, e202308046.
- 50 F. Delogu, *Acta Mater.*, 2008, **56**, 905–912.
- 51 F. Delogu, *Scr. Mater.*, 2013, **69**, 223–226.
- 52 L. Vugrin, M. Carta, S. Lukin, E. Meštrović, F. Delogu and I. Halasz, *Faraday Discuss.*, 2023, **241**, 217–229.
- 53 J. M. Andersen and J. Mack, *Chem. Sci.*, 2017, **8**, 5447–5453.
- 54 R. Rana, N. Hopper, F. Sidoroff, J. Cayer-Barrioz, D. Mazuyer and W. T. Tysoe, *Tribol. Lett.*, 2024, **72**, 76.



- 55 C. Delle Piane, S. Piazzolo, N. E. Timms, V. Luzin, M. Saunders, J. Bourdet, A. Giwelli, M. Ben Clennell, C. Kong, W. D. A. Rickard and M. Verrall, *Geology*, 2017, **46**, 163–166.
- 56 F. Delogu, R. Orrù and G. Cao, *Chem. Eng. Sci.*, 2003, **58**, 815–821.
- 57 A. H. Hergesell, C. L. Seitzinger, J. Burg, R. J. Baarslag and I. Vollmer, *RSC Mechanochem.*, 2025, **2**, 263–272.
- 58 J. F. Reynes, V. Isoni and F. García, *Angew. Chem., Int. Ed.*, 2023, **62**, e202300819.
- 59 H. Mio, J. Kano and F. Saito, *Chem. Eng. Sci.*, 2004, **59**, 5909–5916.
- 60 A. Z. Juhasz and L. Opoczky, *Mechanical Activation of Minerals by Grinding: Pulverizing and Morphology of Particles*, Ellis Horwood Ltd, Chichester, 1977.
- 61 J. Batteas and T. Friščić, *RSC Mechanochem.*, 2025, **2**, 175–177.
- 62 Retsch GmbH, *Operating Instructions Ball Mills: Type PM100/PM200/PM100cm*, Retsch GmbH, Haan, Germany, 2014.
- 63 F. Fischer, K.-J. Wenzel, K. Rademann and F. Emmerling, *Phys. Chem. Chem. Phys.*, 2016, **18**, 23320–23325.

